ISSN 0742-0463, Journal of Volcanology and Seismology, 2026, Vol. 20, No. 2, pp. 114–126. © Pleiades Publishing, Ltd., 2026.

Hydrogeological Conditions and Discharge Regime of the Verkhne Paratunsky Thermal Springs

N. B. Zhuravlev[a], A. V. Kiryukhin[a, *], P. O. Voronin[a], A. V. Sergeeva[a], Bo Feng[b], I. A. Nuzhdaev[a], and Siqing He[b]

[a] *Institute of Volcanology and Seismology, Far East Branch, Russian Academy of Sciences, Petropavlovsk-Kamchatsky, 683023 Russia*

[b] *Jilin University College New Energy and Environment, Changchun, 130021 China*

**e-mail: AVKiryukhin2@mail.ru*

Received October 28, 2025; revised October 28, 2025; accepted December 26, 2025

Abstract—The Verkhne Paratunsky thermal springs are the large natural discharge zone of the Verkhne Paratunsky low-temperature nitrogen geothermal field (Kamchatka, Russia). Their hydrothermal and hydrogeochemical history, as well as their discharge conditions, were analyzed based on previous (1966–1996) and renewed (2024–2025) monitoring of the spring regime. The experimental and operational releases at the Verkhne Paratunsky geothermal field in 1975–1984 led to a significant change in the discharge parameters: a decrease in the maximum temperature of the springs from 67 to 46°C and a decrease in the total mineralization (a 2–2.5-fold decrease in Cl and SO_4), while the flow rates of the entrained springs (3.5–8.2 L/s) are close to the initial values before the start of tests. The flow tests carried out at the Verkhne Paratunsky geothermal field in 1975–1984 led to a significant change in the discharge parameters: a decrease in the maximum temperature of the main springs from 70 to 30–35°C, a decrease in the flow rate from 7.7 to 2.9 kg/s, and a decrease in the mineralization by two times or more (all in average annual terms). By 2025, the flow rates of the main captured springs had recovered to 5 kg/s, the temperature to 49°C, and the mineralization to 50–65% of the initial value. Using the chloride tracer method, an updated assessment of the deep component of the total discharge of the Verkhne Paratunsky springs was estimated varying from 6.3 kg/s (March) to 21.9 kg/s (May) in the annual cycle.

Keywords: Verkhne Paratunsky, thermal springs, flow rate, temperature, mineralization, mode, operation, recovery, monitoring, chloride tracer method, seasonality

DOI: 10.1134/S0742046326700090

INTRODUCTION

The Verkhne Paratunsky geothermal field (Kiryukhin et al., 2025) is located in the Paratunka River valley (Kamchatka Krai, Russia) in the Advanced Special Economic Zone "Kamchatka" and associated Three Volcanoes Park tourism project. The Verkhne Paratunsky springs considered in this study are the largest visible area of natural discharge of the Verkhne Paratunsky geothermal field. It is planned to create the balneological resort Sopka Goryachaya on this territory, as well as to connect the greenhouse complexes of the settlements of Paratunka and Termalny, along with other planned facilities, to the geothermal heating system.

The implementation of these plans involves drilling new production wells and using submersible pumps in existing ones to increase water extraction at the field. Intensification of thermal water extraction can significantly lower the regional piezometric level and lead to a decrease in the flow rate of springs or their complete disappearance, as well as the formation of depression funnels with involvement of waters of external genesis: sea, cold ground, anthropogenically polluted, etc.

Analysis of the conditions of water and heat supply of thermal springs, as well as consideration of the impact of geothermal field operation on the current thermohydrodynamic regime, is critically important for developing strategies for the sustainable operation of the Verkhne Paratunsky field in order to prevent the above-mentioned negative impacts on the quality of thermal waters.

The objectives of this work are: (1) to compare the current regime of the Verkhne Paratunsky springs with the observation period of 1966–1996 to assess the impact of thermal water extraction and changing water supply conditions and (2) analyze the formation conditions of the Verkhne Paratunsky springs.

DISCHARGE CONDITIONS OF THE VERKHNE PARATUNSKY SPRINGS AND ASSESSMENT METHODS

Data on the water regime and chemical composition for the period 1966–1996 were obtained from the hydrogeological yearbooks of the Kamchatka Branch of the Territorial Geological Information Fund for the Far Eastern Federal District.

In October 2024, after a 29-year hiatus, the authors resumed regular (monthly) monitoring observations at the Verkhne Paratunsky thermal springs to determine their current discharge regime. The following were conducted during the monitoring:

1. Measurement of temperature and discharge (using the volumetric method) of thermal springs 3, 10, and 19 (Fig. 1) and water and gas sampling from them. Spring temperatures were measured with an IUCHI 2455 digital thermometer equipped with a type K thermocouple. The discharge of springs drained by thermal pools was measured volumetrically using a 5 L cylindrical container. Water samples were collected in 1.5 L plastic bottles, and gas samples were collected by displacement into 100 mL glass bottles with rubber stoppers.

2. Measurement of the total discharge of the Verkhne Paratunsky springs at the outlet using the chloride tracer (CT) method (Kiryukhin et al., 2024) with a HOBO U24 electrical conductivity logger and injections of 500 g of table salt diluted in 5 L of water. Application of the CT method for determining the deep thermal component of the total discharge in streams is described in (Kiryukhin et al., 2022, 2023, 2025) and is patent protected. A brief description of the specifics of applying this method to assess the total discharge of the Verkhne Paratunsky geothermal springs is provided below.

For continuous recording of the concentration of chloride ion at the outlet of the discharge of the Verkhne Paratunsky springs (see Fig. 1) based on the electrical conductivity of the solution, a HOBO U24-001 logger (full range 0–2500 μS/cm with a recording interval set to 10 s) was used. The peak values of the electrical conductivity of the solution into chloride concentrations was performed using an empirical formula, which was substatiated by calibrating a volumetric water sample (5 L) at the outlet of the Verkhne Paratunsky springs:

$$C = 0.3EC, \quad (1)$$

where C is the chloride ion concentration (ppm) and EC is the electrical conductivity (μS/cm).

Discharge at river point Q_r, the dependence of the change in the tracer concentration in the river on time $C(t)$ during the time interval of tracer movement ($t1$, $t2$), and the mass of the tracer M (chloride ion) are related by the following mass balance formula:

$$M = Q_r \int_{t1}^{t2} C(t)\,dt. \quad (2)$$

In Eq. (2) $C(t) = C_r(t) - C_b(t)$ is the pulse component of the tracer concentration, which is the difference between $C_r(t)$ (concentration of tracer in the river) and $C_b(t)$ (background trend of tracer concentration in the river). With a known mass of the tracer (the runs were carried out with samples of 0.5 kg NaCl or 0.3035 kg chlorine ion), formula (2) can be used to estimate the flow rate at the outlet Q_r:

$$Q_r = \frac{M}{\int_{t1}^{t2} C(t)\,dt}. \quad (3)$$

Based on the flow rate Q_r at the outlet and the concentration of chlorine ion in it, measured analytically, the mass flow rate of chlorine ion is calculated, which can then be recalculated to the mass flow rate of the discharge of the parent geothermal fluid. The concentration of chloride ion in the parent geothermal fluid is taken equal to the maximum concentration detected in thermal springs or nearby wells.

The Paratunsky geothermal area is located 40 km southwest of Petropavlovsk-Kamchatsky (see Fig. 1a) and includes two large geothermal fields: the Paratunsky and Verkhne Paratunsky. The geothermal area is located in a volcanic–artesian basin: the Paratunsky graben with a NNE strike.

The Verkhne Paratunsky springs (see Fig. 1c) are the largest visible natural discharge site at the Verkhne Paratunsky field. The springs emerge on the northeastern slope of Goryachaya Sopka at elevations of 130–150 m above sea level. It is hypothesized that the springs are associated with intersection of the Northern sublatitudinal fault and a submeridional fault along the eastern slope of Goryachaya Sopka (Pavlova, 1979) within the complex of brecciated rocks of the Vilyuchinsky Formation. The springs are confined to an area of 0.017 km^2 (see Fig. 1c). In total, there are up to 13 concentrated thermal spring outlets, some of which form from the mixing of thermal fracture–vein waters and cold groundwater.

Natural thermal manifestations similar to the Verkhne Paratunsky springs are found in hydrogeological massifs composed of crystalline rocks in tectonomagmatic activation zones (Kononov, 1983). For example, the natural discharge of the Gannan geothermal region (Jiangxi Province, China) is represented by a group of more than 50 thermal springs, predominantly with mineralization from 0.23 to 3.6 g/L (Li and Yang, 1992; Zhang, 2001), formed as a result of deep infiltration of atmospheric precipitation followed by leaching of components from Early Cretaceous granites (Xiao et al., 2025). Predominance of N_2 in free gas (91.04–98.0 vol %) (Sun et al., 2004, 2014), the light isotope composition (δD –48.2‰ ~ –36.2‰, $\delta^{18}O$ –7.2‰ ~ –6.5‰) and the temperature at the vent of 38–82°C (Shvartsev et al., 2018) indicate a predominantly meteoric origin of the waters with a contribution from the crustal component (CO_2, He), and elevated (840–1106 m abs.) position of the water recharge (Shi et al., 2024). In the spring regime, a cor-

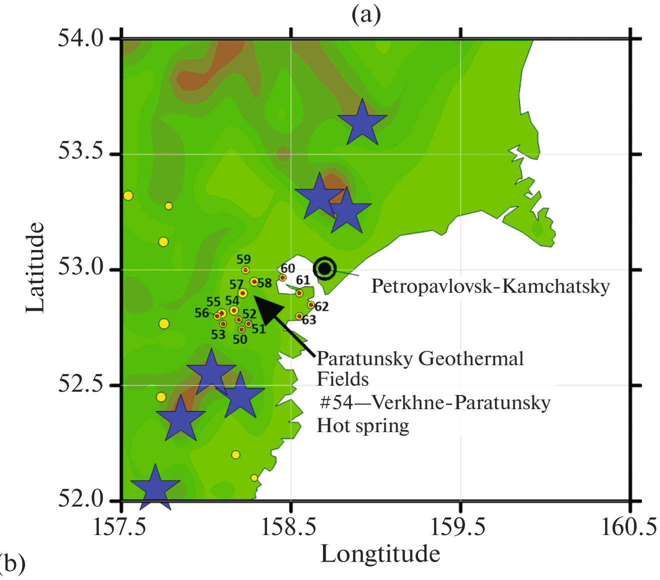

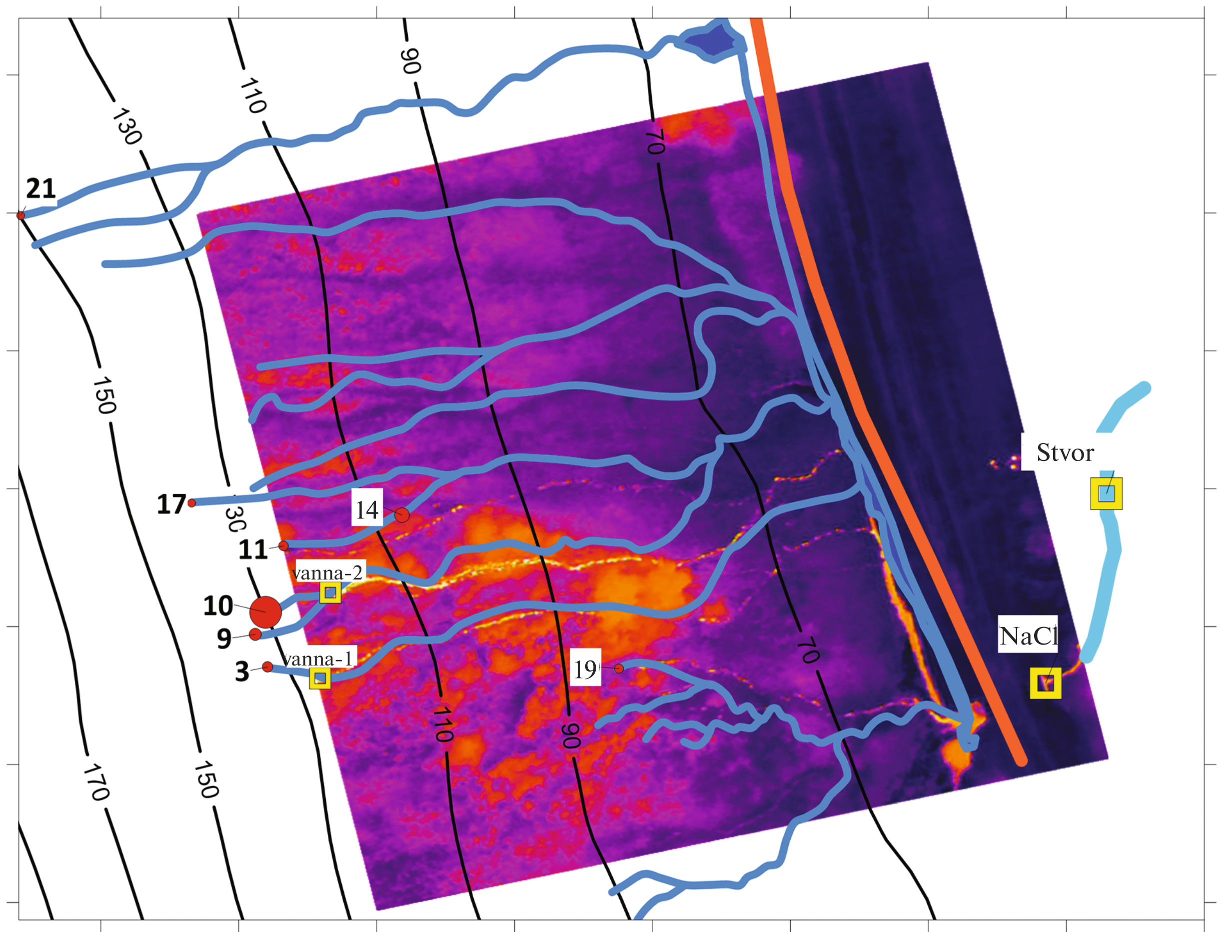

Fig. 1. Location of Verkhne Paratunsky springs (no. 54) in Kamchatka; yellow circles are discharges of low-temperature nitrogen geothermal systems; numerals correspond to catalog (Kiryukhin et al., 2010); blue stars are active volcanoes (a); Verkhne Paratunsky thermal springs: monitoring stations (Vanna-1, Vanna-2), start of tracer (NaCl) and recording of discharge of Verkhne Paratunsky springs at outlet (Stvor), 50 m axis marking (b); perspective infrared image (left) and its interpretation (right) (c).

(c)

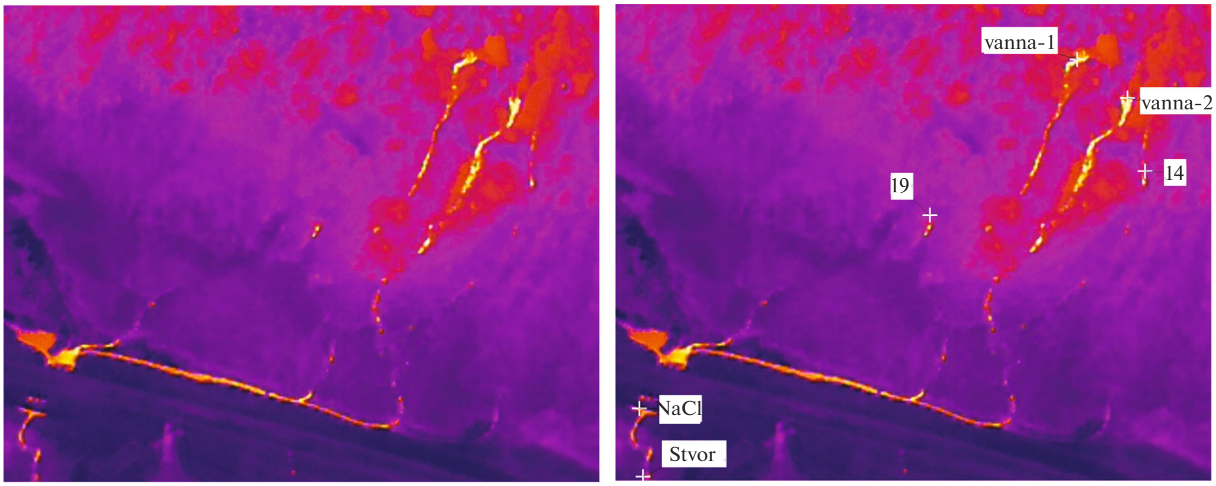

Fig. 1. (Contd.)

relation is observed between the parameters of their discharge (temperature, total mineralization, HCO_3, CO_2, He content) and the seismic activity of the NNE-trending fault zone, to which the natural thermal manifestations of the region are confined (Xiao et al., 2025).

In September 2024, aerial photography was conducted in the area of the Verkhne Paratunsky hot springs using a DJI Mavic 3T drone (China) equipped with wide-angle and thermal imaging cameras. The technical characteristics of the drone are presented on the website (https://aeromotus.ru/product/dji-mavic-3-thermal/).

Planned and prospective thermal imaging surveys were carried out in the morning (08:00 LT) at an altitude of 100 m above the main discharge area. The resulting images were processed using DJI Thermal Analysis Tool 3 and Agisoft Metashape Professional software. It has been determined that the entire flow of the Verkhne Paratunsky springs is collected in a single artificial pipeline under a new backfill road (see Figs. 1b, 1c), which makes it possible to monitor the total discharge at a single outlet, which was selected 60 m below the throughput pipeline indicated above.

Based on the results of exploratory drilling and well testing (Pavlova, 1975; Maltseva, 1993; Danilin, 1995) and subsequent 3D thermohydrodynamic (TH) modeling (Kiryukhin et al., 2025), the following hydrogeological and geothermal conditions are assumed in the discharge area of the Verkhne Paratunsky springs, depicted on the vertical sublatitudinal cross-section (Fig. 2).

CHEMICAL, GASEOUS, AND ISOTOPE COMPOSITION OF THERMAL WATERS OF THE VERKHNE PARATUNSKY SPRINGS

The chemical composition of the thermal spring waters is presented in Table 1 and on the Piper diagram (Fig. 3b). The discharge waters are slightly mineralized (<1.5 g/L), slightly alkaline, calcic–sodic from chloride–sulfate to chloride–hydrocarbonate. The Giggenbach diagram (see Fig. 3a) shows their "immature" character in relation to the chlorite–mica–feldspar equilibrium and is simultaneously an indicator of intensive circulation in the hydrothermal system.

In chemical composition and temperature, the thermal waters of the Sredny site of the Paratunsky field are close to the Verkhne Paratunsky springs, with slightly higher mineralization, lower pH, comparable concentrations of anions, silica, and arsenic. The biggest difference between them is in the ratio of anions: the Verkhne Paratunsky waters are more chloride-rich, while the waters of the Sredny–Paratunsky section are almost entirely sulfate-rich (~86% eq.).

The free gas of the Verkhne Paratunsky springs is dominated by nitrogen (93–95%), oxygen (5%), argon, carbon dioxide, and helium are also present (Table 2).

The microcomponent chemical composition of the Verkhne Paratunsky springs is presented in Table 3. The following microcomponents were detected in mg/L: strontium (0.31–0.58 mg/L), arsenic (0.14–0.29 mg/L), barium (0.008–0.104 mg/L), and manganese (0.01–0.06 mg/L).

Arsenic, strontium, and barium indicate that the springs are fed by deep origin thermal waters, most likely alkaline, as, e.g., at the Pauzhetsky steam–hydrothermal field, which also contains arsenic

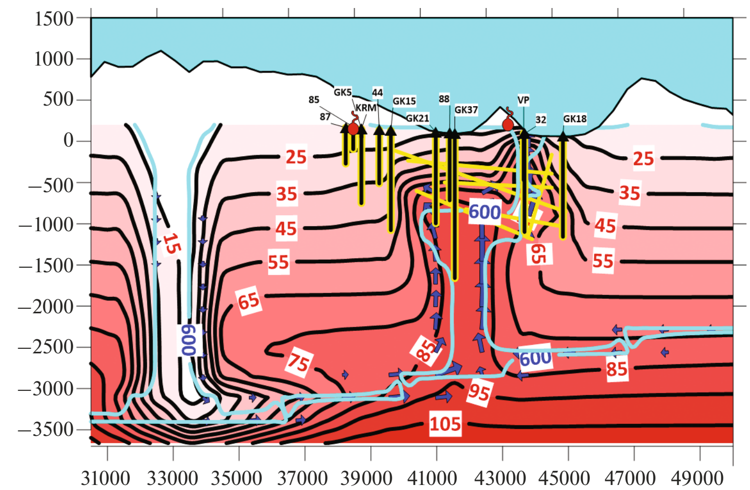

Fig. 2. Vertical section of three-dimensional TH model (Kiryukhin et al., 2025, scenario no. 2). VP, Verkhne Paratunsky springs; KRM, Karymshinsky springs; red numbers, temperature, °C; blue numbers, NaCl distribution, ppm; blue arrows, vectors proportional to flow rates of thermal fluid; yellow lines, traces of productive faults.

(Sergeeva et al., 2024). In alkaline solutions, arsenic becomes mobile and transforms into arsenite or arsenate forms.

The isotope composition of thermal waters of the Verkhne Paratunsky springs is shown in Fig. 4. The waters are heavier ($-110‰ < \delta D < -104‰$, $-15.4‰ < \delta^{18}O < -14.3‰$) compared to N, NP, and M Sites of the Paratunsky field ($-116‰ < \delta D < -110‰$, $-16‰ < \delta^{18}O < -15‰$). The waters of the Karymshina and Paratunka rivers, which are fed by groundwater horizons, are even heavier in isotope composition ($-100‰ < \delta D < -95‰$, $-14.3‰ < \delta^{18}O < -13.2‰$).

ANALYSIS OF THE HYDROGEOLOGICAL REGIME OF VERKHNE PARATUNSKY SPRINGS

According to the thermohydrodynamic characteristics of discharge and conditions of water recharge, the Verkhne Paratunsky springs are divided into two types (Pavlova, 1979):

Type 1. Thermal springs 3, 9, 10, and 14 are fed by thermal waters circulating in fracture–vein systems associated with the aquifer complex of volcanogenic-sedimentary rocks of the Vilyuchinsky Formation; they discharge from fractured hydrothermally altered rocks. Currently, springs 3, 9, and 10 are drained by two thermal pools (Vanna-1, Vanna-2, see Fig. 1c), which are popular balneological facilities.

Type 2. Thermal springs 11 and 19, whose water recharge is of a mixed nature, are derived from fracture–vein thermal waters from the aquifer complex of the Vilyuchinsky Formation and fracture-fed cold waters from volcanic formations of the Alneysky Formation. The spring outlets are associated with eluvial–deluvial deposits.

Seasonal flow rate patterns. During the winter period (from November–December to mid-April–

Table 1. Chemical composition of waters of Verkhne Paratunsky springs (spring 9), mg/L

Date	pH	HCO_3^-	Cl^-	SO_4^{2-}	F^-	Li^+	Na^+	K^+	Ca^{2+}	Mg^{2+}	H_3BO_3	SiO_2
October 15, 2024	7.4	24.4	72.7	329.2	1.9	0.5	159.4	2.8	52.0	0.1	21.9	49.5
November 15, 2024	7.0	23.2	72.7	311.9	2.0	0.5	149.1	2.9	49.2	0.1	22.1	54.4
December 15, 2024	6.1	24.4	74.5	319.9	2.0	0.4	149.5	2.8	52.8	0.5	21.3	59.3
January 20, 2025	7.0	25.6	74.4	287.2	2.1	0.4	141.8	2.9	50.2	0.2	22.3	64.2
February, 2025	8.1	26.5	78.0	305.9	1.8	0.5	141.8	2.9	45.3	0.2	21.7	46.2
March 21, 2025	7.1	24.4	78.0	313.0	2.2	0.4	140.3	2.2	49.1	0.1	21.8	53.0
April 21, 2025	7.9	28.0	77.2	345.0	2.1	0.4	153.0	2.8	56.5	0.3	23.1	34.9
May 16, 2025	8.2	24.8	78.0	316.0	2.2	0.4	151.8	2.6	52.0	0.2	19.8	32.4
June 16, 2025	7.4	24.4	69.5	298.0	2.03	0.4	126.4	2.6	54.1	0.1	20.3	39.1
July 18, 2025	8.0	24.4	66.0	280.1	2.0	0.5	162.1	2.6	38.3	0.1	18.8	36.2

Chemical analyses were carried out at the Analytical Center, Institute of Volcanology and Seismology, Far East Branch, Russian Academy of Sciences.

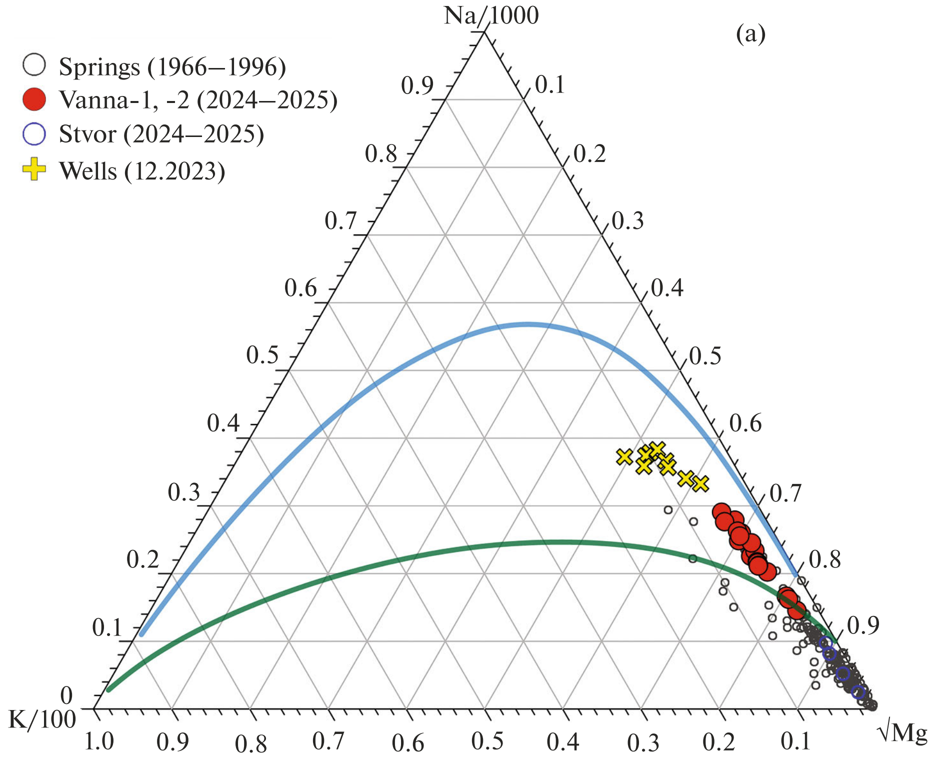

Fig. 3. Giggenbach (a) and Piper (b) diagrams for waters of Verkhne Paratunsky thermal springs and thermal waters of the field, encountered by wells.

early May), the flow rates of all types of springs decrease, consistent with the general decrease in the flow rates of streams during the low-water period in the region. The minimum flow rates of the springs are reached at the end of the winter low water period, but are sometimes recorded earlier (January–March) or later (May). There is usually no coincidence between the dates of minima according to different springs; the difference between them ranges from several days to several months.

When snowmelt starts, the flow rates of all thermal springs begin to experience an intensive rise. According to monitoring data, the maximum flow rates of the springs are ahead of peak flood of the Paratunka River and maximum levels of thermal waters in geothermal wells; the difference between them is from 5–10 days to 1–1.5 months, and the amplitudes of the spring increase in flow rates are 0.29–12.4 L/s (Pavlova, 1979).

Seasonal temperature patterns. Prior to 1975, the minimum annual average weighted temperatures in the springs occurred in the spring–summer period and coincided with an increase in their flow rate (Fig. 5).

The above-mentioned seasonal patterns of increased total flow rate and decreased average weighted temperature of the Verkhne Paratunsky

Table 2. Composition of free gas of Verkhne Paratunsky thermal springs, vol %

Date	He	O_2	N_2	Ar	CO_2	CH_4
January 20, 2025	0.037	4.39	94.486	0.54	0.443	<0.001
February 17, 2025	0.038	4.284	94.616	0.69	0.172	<0.001
March 21, 2025	0.038	4.829	94.188	0.695	0.127	<0.001
April 21, 2025	0.038	5.795	93.266	0.717	0.076	<0.001
June 16, 2025	0.037	4.672	94.691	0.542	0.055	<0.001
July 18, 2025	0.033	6.311	92.951	0.329	0.31	<0.001
August 20, 2025	0.034	4.968	94.365	0.568	0.002	<0.001

Gas composition analyses were carried out at the Analytical Center, Institute of Volcanology and Seismology, Far East Branch, Russian Academy of Sciences.

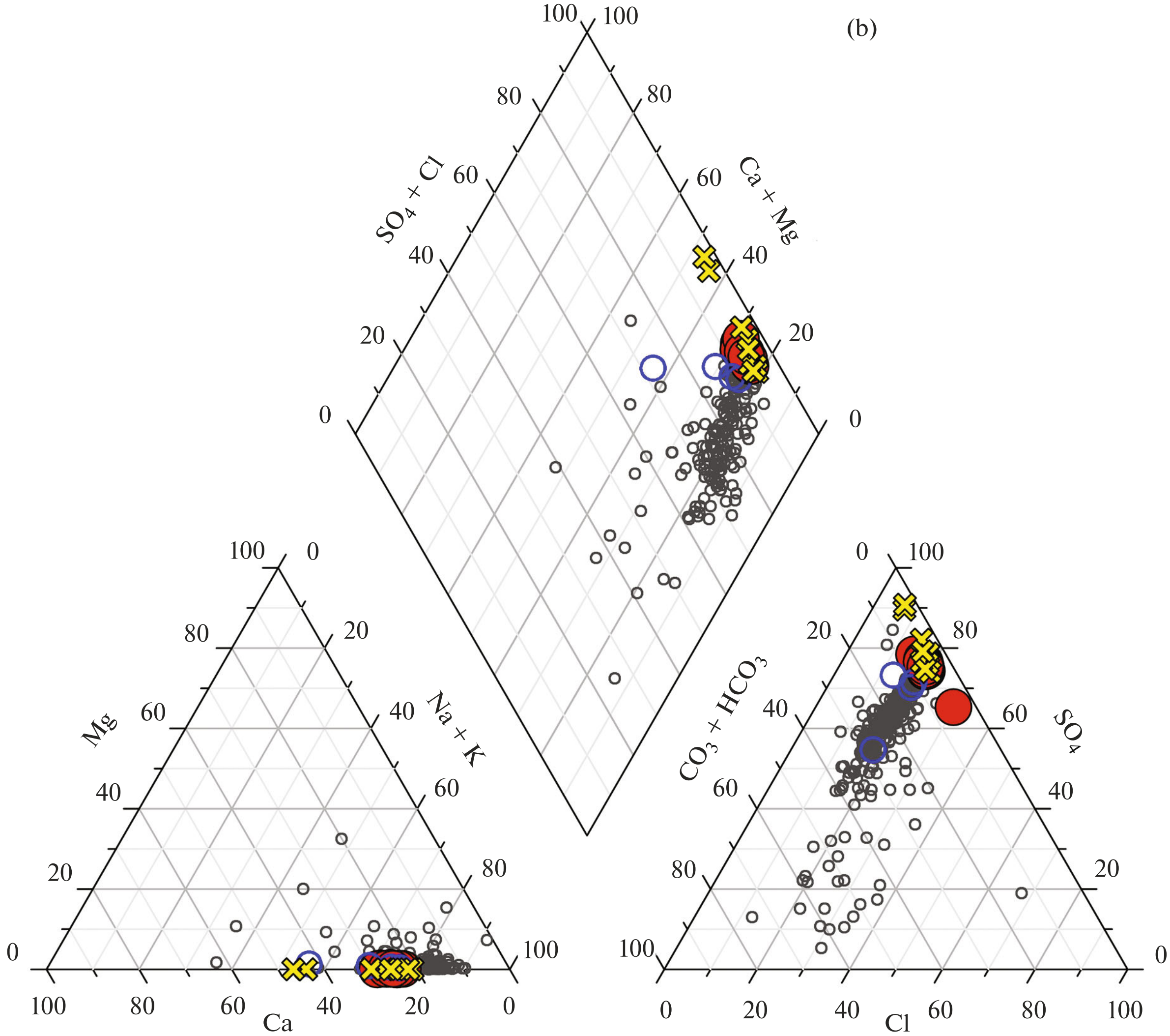

Fig. 3. (Contd.)

springs are reproduced by a thermohydrodynamic model (Kiryukhin et al., 2025, Section 6.2.3, Fig. 10), which shows that the increase in the discharge of thermal waters during the spring–summer flood period is caused by local ground water level rise and simultaneous dilution in the discharge areas (May–June).

Long-term flow rate patterns. Long-term changes in the regime of the Verkhne Paratunsky springs are shown in Fig. 5. The flow rates of springs in a state undisturbed by operation (before 1975) were characterized by the following average long-term values: the Type 1, from 0.79 (spring 3) to 4.8 L/s (spring 10); the Type 2, 0.40–1.12 L/s (spring 19). The total visible discharge of thermal springs 3, 9, and 10 before the start of operation of the Verkhne Paratunsky field was 7–9 kg/s at a temperature of 60–65°C (Pavlova, 1979).

Well Flow Tests (WFT) at the Verkhne Paratunsky field were carried out in the periods 1971–1972, 1975–1979, and 1982–1984 (see Fig. 5) (Maltseva, 1993). During the 1971–1972 WFT, water withdrawals ranged from 93 to 136 L/s. The highest water withdrawal occurred during the WFT of 1975–1980, when the flow rate was maintained in the range of 251–310 L/s for 44 months. During the WFT period 1982–1984, the average monthly flow rate was 246–312 L/s, and the maximum average annual flow rate in 1983 was 283 L/s. The unevenness of the change in flow rate during the WFT period was due to the commissioning of new wells or shutdown of wells, as well as the spontaneous discharge of drilled wells. WFTs at the Verkhne Paratunsky field had a significant impact on the regime of Type 1 springs. During WFT periods, the flow rates of the springs decreased and their operation ceased (springs 3, 9, 10, 14).

Long-term temperature patterns. The average annual temperature of springs of the Types 1 and 2 over the long-term period of 1983–1996 decreased by 3–29 and 11–18°C, respectively. The decrease in tem-

Table 3. Microcomponent composition of Verkhne Paratunsky thermal springs, mg/L

Place	Date	Ba	As	Sr	Mn
Verkhne Paratunsky springs, Vanna-1	January 20, 2025	0.0493	0.292	0.240	0.0642
Verkhne Paratunsky springs, Vanna-1	February 15, 2025	0.1041	0.254	0.284	0.0128
Verkhne Paratunsky springs, Vanna-1	March 21, 2025	0.0063	0.258	0.584	<0.005
Verkhne Paratunsky springs, Vanna-1	April 21, 2025	0.0047	0.229	0.416	<0.005
Verkhne Paratunsky springs, Vanna-1	May 16, 2025	<0.005	0.255	0.379	<0.005
Verkhne Paratunsky springs, Vanna-1	June 16, 2025	<0.005	0.220	0.225	<0.005
Verkhne Paratunsky springs, Vanna-1	July 18, 2025	<0.005	0.222	0.349	<0.005
Verkhne Paratunsky springs, Vanna-2	January 20, 2025	0.0239	0.330	0.243	0.0734
Verkhne Paratunsky springs, Vanna-2	February 15, 2025	0.0351	0.267	0.265	0.0054
Verkhne Paratunsky springs, Vanna-2	March 21, 2025	0.0044	0.259	0.565	<0.005
Verkhne Paratunsky springs, Vanna-2	April 21, 2025	0.0052	0.255	0.312	<0.005
Verkhne Paratunsky springs, Vanna-2	May 16, 2025	<0.005	0.216	0.379	<0.005
Verkhne Paratunsky springs, Vanna-2	June 16, 2025	<0.005	0.216	0.187	<0.005
Verkhne Paratunsky springs, Vanna-2	July 18, 2025	<0.005	0.230	0.344	<0.005

The analyses were carried out at the Analytical Center, Institute of Volcanology and Seismology, Far East Branch, Russian Academy of Sciences.

Table 4. Results of measuring total discharge of Verkhne Paratunsky thermal springs and calculation of its deep component using CT method at outlet (see Fig. 1)

Date	Q_r, kg/s	Cl, mg/L	CL, g/s	Q_d, kg/s	## logger	
December 24, 2024	6.4	74.5	0.48	6.1	20256223	Vanna-2
January 20, 2025	20.1	28.4	0.57	7.3	20256223	Stvor
January 20, 2025	19.3	28.4	0.55	7.0	21790695	Stvor
March 21, 2025	15.4	31.9	0.49	6.3	20256223	Stvor
April 21, 2025	38.2	17.6	0.67	8.6	20256223	Stvor
May 16, 2025	194.9	8.77	1.71	21.9	20256223	Stvor
July 18, 2025	55.9	15.3	0.86	11.0	20256223	Stvor
August 20, 2025	33.1	21.27	0.70	9.0	20256223	Stvor

The concentration of chloride ion in the parent fluid was taken as 78 mg/L (see Table 1).

perature of the Type 1 springs is due to a decrease in their flow rate and, as a consequence, an increase in temperature losses along the filtration paths. The smaller decrease in water temperature in the Type 2 springs is due to the fact that surface and ground cold waters always occupy a significant place in their recharge.

Not a single spring saw previous temperatures restored by 1996 (see Fig. 5). Even by 2025, more than 40 years after completion of the WFT, the temperature regime of the thermal springs had not recovered to the values in the undisturbed state (1966).

Long-term chemical composition patterns. Hydrodynamic and temperature changes in the springs were accompanied by changes in the chemical composition of water. For all springs, during the WFT period, there was a decrease in mineralization at the expense of the entire macrocomponent composition.

Based on the comparison of long-term changes in the flow rate, temperature, and mineralization of the Verkhne Paratunsky springs with WFT periods, it can be concluded that extraction of thermal waters via the wells of the Verkhne Paratunsky field intercepts and reduces the natural discharge of the springs with a decrease in their mineralization and temperature.

2024–2025 monitoring results. Figure 6 plots in hydrological year format the changes in the deep component of discharge Qd (Table 4) and flow rates of Type 1 springs (Table 5) based on the results of the resumed monitoring in 2024–2025.

The CT method made it possible to estimate the total discharge of the Verkhne Paratunsky springs at the outlet (see Fig. 6, Table 4). In the deep component Qd, estimated based on the maximum chlorine concentration ion of 78 mg/L in spring 10 (see Table 1), it changes in the annual cycle from 6.3 (March) to

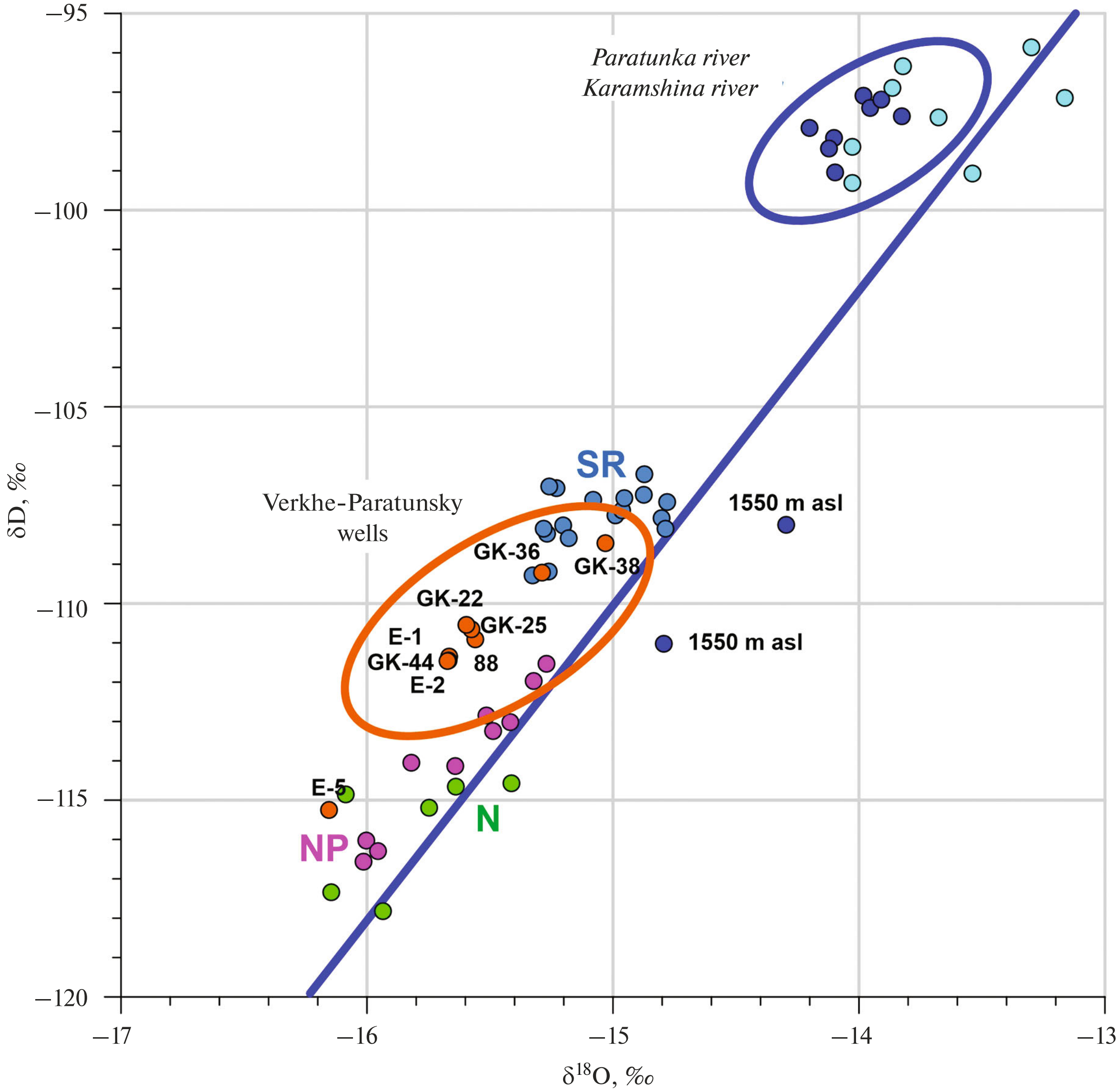

Fig. 4. Isotope composition of waters of Verkhne Paratunsky field during low water period of December 2023. Numerals next to circles correspond to well numbers. Circles of other colors are samples taken during low-water period (September 2016) (Kiryukhin et al., 2017): purple, Nizhne-Paratunsky (NP) site; green, Northern (N) site; gray, Sredny (SR) site (Kiryukhin et al., 2025). isotope composition of waters was analyzed by I.V. Tokarev using Picarro L2120-i laser infrared spectrometer in high-performance mode at RDMI Research Center, St. Petersburg State University Science Park, and by P.O. Voronin using IWA-35EP isotope analyzer at the Heat and Mass Transfer Laboratory of the Institute of Volcanology and Seismology, Far East Branch, Russian Academy of Sciences.

21.9 kg/s (May). It is possible that the maximum Qd occurs in June (a gap in measurements). The average annual value of the deep component of the natural discharge of the Verkhne Paratunsky springs is 10.2 kg/s.

The flow rate of Type 1 springs increases from 3.5 to 8.2 L/s during the spring–summer flood and decreases during the winter low water period (see Fig. 6, Table 5). The maximum temperature of the springs changes synchronously with an increase from 46 to 58°C, but the maximum temperature is shifted by 2 months compared to the maximum flow rate and falls in August 2025.

DISCUSSION AND CONCLUSIONS

The regime of the Verkhne Paratunsky thermal springs in a state undisturbed by operation (before 1967) (Pavlova, 1979) was characterized by total flow rates of the main springs (3, 9, 10) from 7.6 to 7.8 kg/s, a temperature of about 70°C (Fig. 7), and SO_4 and Cl

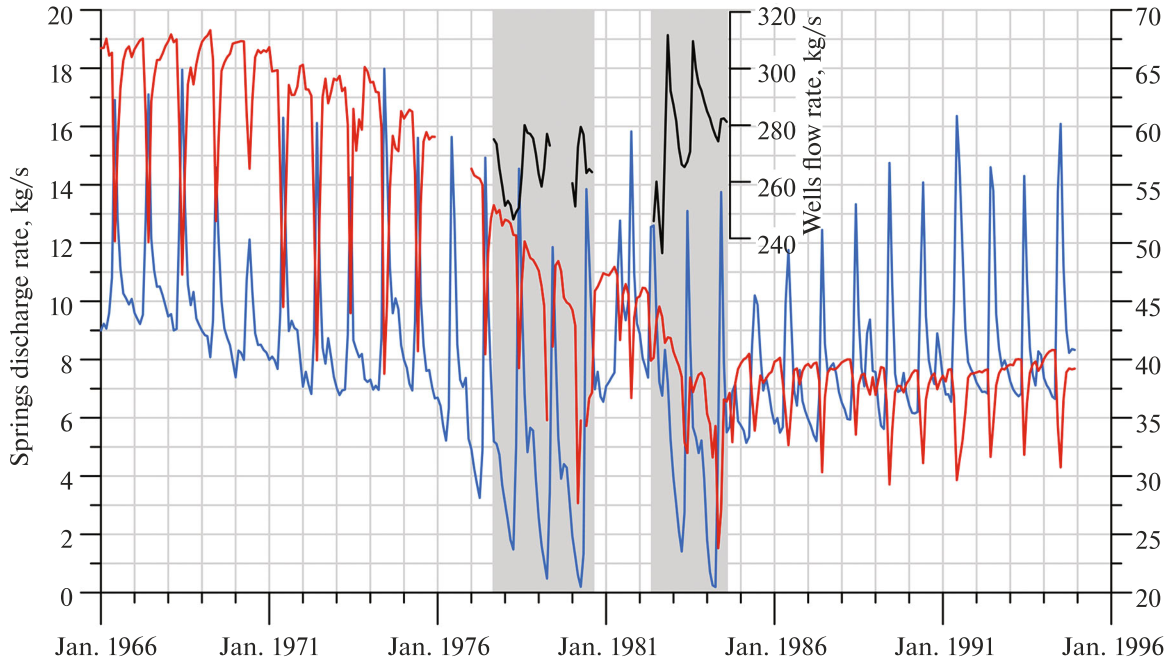

Fig. 5. Variations in total flow rate (blue plots) and average weighted temperature (red plots) of Verkhne Paratunsky thermal springs according to data from (Pavlova, 1975; Danilin, 1995). Gray color shows WFT intervals; total flow rates of experimental wells are shown in kg/s.

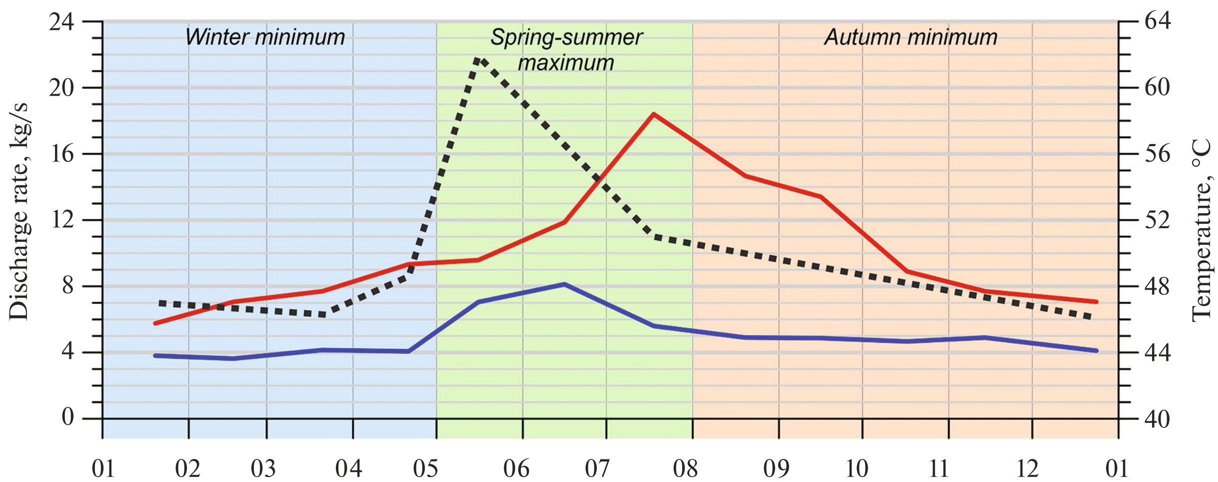

Fig. 6. Graph of changes in flow rate of deep component of total discharge (Q_d), total flow rate, and maximum temperature of springs 3, 9, 10 (Type 1), according to monitoring data for 2024–2025 in hydrological year format. Dotted line is Q_d; blue lines are total flow rate; red lines are maximum temperature.

concentrations of 475 and 125 mg/L, respectively (Fig. 8).

The impact of WFTs (1970–1975, 1981–1983) led to a significant change in the temperature and chemical regime of the main springs (springs 3, 9, 10). During WFT periods, the average flow rates of thermal springs decreased from 7.6–7.8 kg/s in the undisturbed state (1966) to 2.9–3.0 kg/s during the most intensive WFT periods, accompanied by a decrease in temperature at the outlet from 70 to 30–35°C. A decrease in mineralization occurred in all springs for all components. The recovery period after WFT (1980–1982, 1984–2025) is characterized by a more dynamic recovery of discharge rates, compared to the recovery of mineralization and water temperature.

The full recovery of the Verkhne Paratunsky springs has not occurred even after more than 40 years. As of 2025, the thermal springs discharge at an average annual total flow rate of 5 kg/s at a weighted average temperature of 48.9°C. In the average annual release

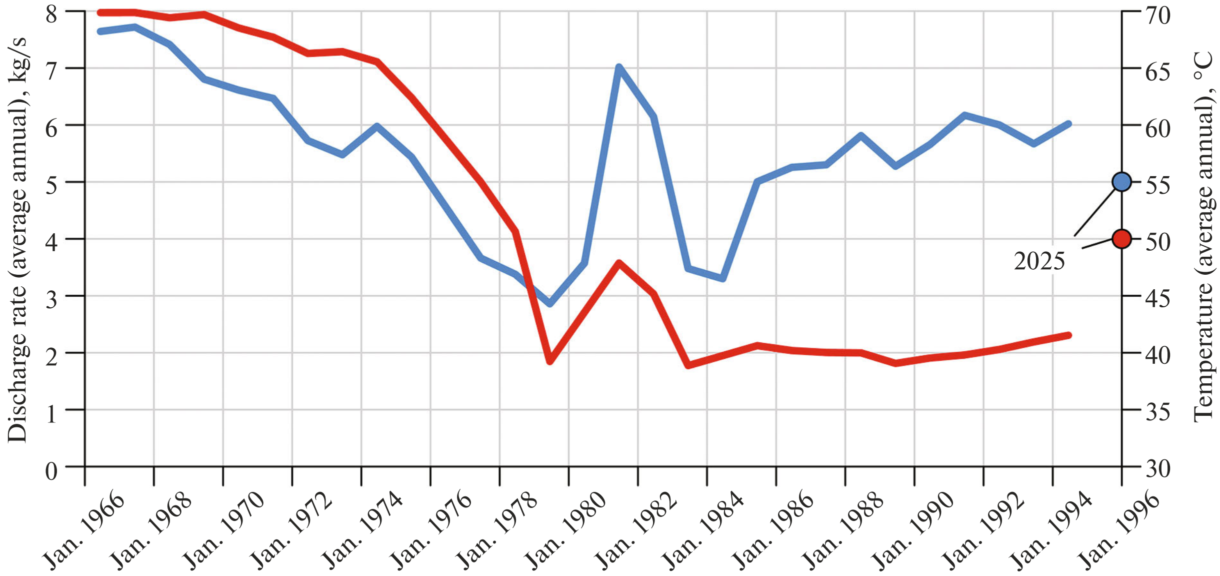

Fig. 7. Changes in total average annual flow rate and average weighted temperature of springs 3, 9, 10 in average annual terms in period 1966–1996 (Pavlova, 1979; Maltseva, 1993; Danilin, 1996). Colored symbols show average annual flow rate (blue) and temperature (red) according to resumed monitoring data in 2025.

for 2025, there was an increase in the Cl and SO_4 contents (see Fig. 8), but it had not yet reached the initial values before the start of operation. The average annual value of the deep component of the natural discharge of the Verkhne Paratunsky springs is estimated by the CT method at 10.2 kg/s (2025). These values provide the initial values of the total average annual flow rate of 7.6 kg/s of the main springs (3, 9, 10) (see Fig. 7), but the 0.79 kg/s of chlorine rate (see Table 4) did not reach the initial 0.96 kg/s (see Figs. 7 and 8) of

Table 5. Field measurement data of temperature *T* and discharge *Q* for springs 3 (Vanna-1), 9+10 (Vanna-2), their combined discharge, and weighted average temperature

Date	*T* spring 3 (Pool 1), °C	*T* spring 9 + 10 (Pool 2), °C	*Q* Pool 1, kg/s	*Q* spring 9 + 10 (Pool 2), kg/c	*Q* total, kg/s	*T* weighted avg., °C
October 17, 2024	48.3	48.9	1.42	3.25	4.67	48.7
November 14, 2024	43.9	47.7	1.51	3.39	4.90	46.5
December 24, 2024	42.0	47.1	1.30	2.81	4.11	45.5
January 20, 2025	44.5	45.8	1.24	2.57	3.81	45.4
February 17, 2025	45.1	47.1	0.91	2.72	3.63	46.6
March 21, 2025	45.8	47.7	1.20	2.95	4.15	47.1
April 21, 2025	45.5	49.3	1.73	2.34	4.07	47.7
May 16, 2025	48.6	49.6	3.66	3.39	7.05	49.1
June 16, 2025	49.7	51.9	4.62	3.51	8.12	50.6
July 18, 2025	54.7	58.4	2.10	3.50	5.60	57.0
August 20, 2025	52.1	54.7	1.68	3.22	4.90	53.8
September 16, 2025	52.1	53.4	1.57	3.30	4.87	53.0
November 21, 2025	43.8	48.3	1.42	2.67	4.09	46.7
December 18, 2025	43.2	47.2	1.48	3.07	4.55	45.9

Temperature measurements of springs were performed using an IUCHI 2455 digital thermometer (Japan) with a KTXA 01.02-002-k1-I-T310-2-1600 (Russia) type K thermocouple measuring the temperature range from –40 to 900°C. The manufacturer's stated thermocouple measurement error is no more than 1.1°C with a 40°C temperature difference at the connector. Measurements were calibrated using two control points: 0°C (ice water mixture at atmospheric pressure at sea level) and 100°C (boiling water at atmospheric pressure at sea level), with the thermocouple held in each medium for 5 min.

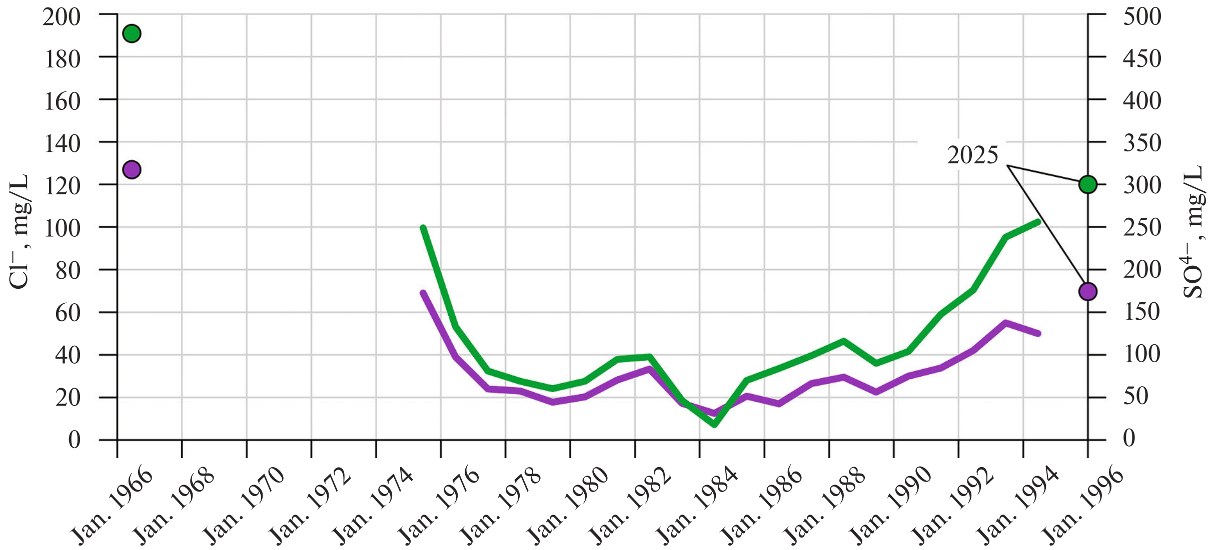

Fig. 8. Change in Cl and SO_4 contents of springs 3, 9, 10 in average annual terms in period 1966–1996 (Pavlova, 1979; Maltseva, 1993; Danilin, 1996). Colored symbols show average annual Cl and SO_4 contents according to resumed monitoring data in 2025.

the Verkhne Paratunsky springs before the start of operation of the geothermal field.

In the annual cycle, according to monitoring data from 2024–2025, the temperature of the main springs (springs 3, 9, 10) varied from 46 to 58°C; chloride ion, from 66 to 78 mg/L; sulfate ion, from 280 to 345 mg/; the total flow rate ranged from 3.5 to 8.2 L/s; deep discharge, from 6.3 to 21.9 kg/s, with maximum values in the postflood period (June–August). This generally corresponds to the patterns of the annual cycle of the main Verkhne Paratunsky springs, established before the start of operation of the geothermal field (Pavlova, 1979).

FUNDING

The study was carried out under topic no. FWME-2024-0007 of the Institute of Volcanology and Seismology, Far East Branch, Russian Academy of Sciences, using the resources of the Shared Research Facility “Kamchatka Center for Elemental, Mineral, and Isotope Analysis” of the IVS FEB RAS.

CONFLICT OF INTEREST

The authors of this work declare that they have no conflicts of interest.

REFERENCES

Antonyuk, M.V., Gvozdenko, T.A., Lebedev, S.V., and Chelnokova, B.I., The state and perspectives for balneological resources of the Sakhalin Region in rehabilitation and sanatorium therapy, *Tikhook. Med. Zh.,* 2023, no. 4 (94), pp. 16–20.

Bodvarsson, G.S., Temperature/flow statistics and thermomechanics of low-temperature geothermal systems in Iceland, *J. Volcanol. Geotherm. Res.,* 1983, vol. 19, pp. 255–280.

Bortnikova, S.B., Gavrilenko, G.M., Bessonova, E.P., and Lapukhov, A.S., The hydrogeochemistry of thermal springs on Mutnovskii Volcano, southern Kamchatka, *J. Volcanol. Seismol.,* 2009, vol. 3, pp. 388–404.

Danilin, A.A., Danilevich, N.S., and Kandinskaya, S.V., (*Izuchenie rezhima podzemnykh vod na uchastkakh opornoi gidrogeologicheskoi seti, reprezentativnom basseine “Plotnikova-Dalniy”, control za okhranoi podzemnykh vod ot istoshcheniya i zagryazneniya i vedenie GVK “Podzemnye vody” na terrotorii Kamchatskoi oblasti v 1993–1996 gg.* (A Study of Groundwater Regime in Segments of the Reference Hydrogeological Network, in the Representative Plotnikova-Dalniy Basin, Monitoring the Protection of Groundwater with Regard to Depletion and Contamination, and Conducting the Podzemnye Vody GVK in the Territory of Kamchatka Region during the Period 1993–1996), Elizovo: Kamch. Terr. Gidroek., 1996, 4 vols.

Giggenbach, W.F., Geothermal solute equilibria. Derivation of Na–K–Mg–Ca geoindicators, *Geochim. Cosmochim. Acta,* 1988, vol. 52, no. 12, pp. 2749–2765.

Kiryukhin, A.V., Kiryukhin, V.A., and Manukhin, Yu.F., *Gidrogeologiya vulkanogenov* (Hydrogeology of Volcanogenes), S. Petersburg: Nauka, 2010. elibrary.ru/item.asp?id=48388631.

Kiryukhin, A.V., Vorozheikina, L.A., Voronin, P.O., and Kiryukhin, P.A., Thermal and permeability structure and recharge conditions of the low temperature Paratunsky geothermal reservoirs in Kamchatka, Russia, *Geothermics*, 2017, vol. 70, pp. 47–61.

Kiryukhin, A.V., Polyakov, A.Yu., Zhuravlev, N.B., Tsuchiya, N., Rychkova, T.V., Usacheva, O.O., and Dubrovskaya, I.K., Dynamics of natural discharge of the hydrothermal system and geyser eruption regime in the Valley of Geysers, Kamchatka, *Geothermics,* 2022, vol. 136. 105 166.

Kiryukhin, A.V., Polyakov, A.Yu., and Usacheva, O.O., *A Device for Estimating the Discharge of Chloride Tracer to Water Streams,* Patent RU 2832424 C1. 2024.

Kiryukhin, A.V., Zhuravlev, N.B., Burnaikin, D.N., and Tokarev, I.V., Conceptual numerical modeling of low-temperature nitrogen geothermal systems on the Verkhne-Paratunsky and Paratunsky fields, *Geothermics*, 2025, vol. 131. Art. 103341.

Kiryukhin, A.V., Sergeeva, A.V., Usacheva, O.O., Lavrushin, V.Yu., and Tokarev, I.V., Thermal-hydrodynamic modeling of the Valley of Geysers and Kikhpinych volcano magma-hydrothermal system, *J. Heat and Mass Transfer,* 2025, vol. 38, no. 1, pp. 127–168.

Kiryukhin, A.V., Nesterenko, M.Yu., and Usacheva, O.O., The 2024 eruption dynamics of the Grot Geyser (Geyser Valley, Kamchatka), *J. Volcanol. Seismol.,* 2025, vol. 19, no. 3, pp. 215–223.

Kononov, V.I., *Geokhimiya termal'nykh vod oblastei sovremennogo vulkanizma (riftovykh zon i ostrovnykh dug)* (The Geochemistry of Thermal Waters in Areas of Present-Day Volcanism: Rift Zones and Island Arcs), Moscow: Nauka, 1983.

Li, X. and Yang, Z., Analysis on the geological structure conditions formed in Jiangxi hot-spring, *J. of East China Geological Institute,* 1992, no. 3, pp. 221–228.

Maltseva, K.I., Nazhalova, I.N., and Raicheva, I.S., *Izuchenie rezhima podzemnykh vod na uchastkakh opornoi gidrogeologicheskoi seti, reprezentativnom basseine "Plotnikova-Dalniy"* (A Study of Groundwater Regime in Segments of the Reference Hydrogeological Network, in the Representative Plotnikova-Dalniy Basin). A Multiyear Report on the Study of Groundwater Behavior in the Territory of Kamchatka Region during the Period 1986–1990, Termalny: GGP Kamchatgeologiya, 1993, 5 vols.

Pavlova, L.E., Efremova, L.A., and Novikova, E.V., *Svodnyi otchet po izucheniyu rezhima podzemnykh vod na territorii Kamchatskoi oblasti za period 1964–1975 gg.* (A Summary Report on the Study of Groundwater Behavior in the Territory of Kamchatka Region for 1964-1975), Elizovo: Kamch. Terr. Gidrog. Upravl., 1979, 5 vols.

Sergeeva, A.V., Rychagov, S.N., Kravchenko, O.V., Sandimirova, E.I., Nazarova, M.A., Kartasheva, E.V., and Kuzmina, A.A., Mineral and geochemical features of zeolite-siliceous deposits at the Pauzhetka Geothermal Field, southern Kamchatka, *J. Volcanol. Seismol.,* 2024, vol. 18, no. 1, pp. 32–47. https://doi.org/10.31857/S0203030624010045

Shi, X., Bai, X., Sun, Z., Liu, J., Ye, H., Pang, L., Guan, Y., and Chen, G., Hydrogeochemical characteristics of the typical mid-temperature hot springs in northern and southern Jiangxi, *Bull. of Mineralogy, Petrology and Geochemistry,* 2024, vol. 43, no. 3, pp. 521–532.

Shvarts, Ya.B., Nurmukhamedov, A.G., Vorozheikina, L.A., Kostenko, N.P., Rozhkov, A.M., Dekusar, Z.P., Skorobogatsko, L.S., and Sokolokov, V.A., *Opytno-metodicheskaya rabota po primeneniyu geologo-strukturnykh, gidrogeologicheskih, geofizicheskikh i distantsionnykh kriteriev poiska termalnykh vod na zakrytykh ploshchadyakh. Otchet Avachinskoi tematicheskoi gidrogeologicheskoi partii o rezultatakh rabot, provedennykh na Petropavlovskoi ploshchadi v 1989–1995 gg.* (Experimental Methodological Work to Apply Geological-structural, hydrogeological, Geophysical, and Distance Criteria in the Search for Thermal Waters in Closed Areas. A Report of the Avachinsky Topical Hydrogeological Team on the Results of the Operations Performed in the Petropavlovsk Area in 1989–1995), Termalny: TOO Akva, 1995, 5 vols.

Shvartsev, S.L., Zamana, L.V., Plyusnin, A.M., and Tokarenko, O.G., Equilibrium of nitrogen-rich spring waters of the Baikal Rift Zone with host rock minerals as a basis for determining mechanisms of their formation, *Geochemistry International,* 2015, vol. 53, no. 8, pp. 713–725.

Shvartsev, S.L., Sun, Z., Borzenko, S.V., Gao, B., Tokarenko, O.G., and Zippa, E.V., Geochemistry of the thermal waters in Jiangxi Province, China, *Applied Geochemistry*, 2018, vol. 96, pp. 113–130.

Smirnova, N.F. and Zakharova, G.S., *Otchet o zavershayushchikh rabotakh na Verkhne-Paratunskom mestorozhdenii termalnykh vod, provedennykh v 1980–1981 gg. (detalnaya razvedka Verkhne-Paratunskogo mestorozhdeniya termalnykh vod)* (Report on the Terminal Work at the Verkhe-Paratunsky Thermal Water Field Carried out in 1980-1981: Detailed Exploration of the Verkhne-Paratunsky Thermal Water Field), Termalny: Parat. Gidrogeol. Eksped., 1981.

Sun, Z., Gao, B., and Liu, J., Geothermal gas geochemistry of the Hengjing hot springs area in Jiangxi province, *Geoscience,* 2004, no. 1, pp. 116–120.

Sun, Z., Gao, B., and Zhang, Z., Isotopic and geochemical evidence for origin of geothermal gases from hotsprings in southern Jiangxi Province, SE-China, *Chinese J. of Geology (Scientia Geologica Sinica),* 2014, vol. 49, no. 3, pp. 791–798.

Xiao, F., Zhou, Y., Zhang, S., Qi, X., and Xiao, W., Geochemical characteristics of hot spring fluids in the Xunwu-Shicheng fault zone of southern Jiangxi, *Hydrogeology and Engineering Geology,* 2025, vol. 52, no. 2, pp. 203–216.

Zhang, W., Application of hydrogeochemical method to the origin analysis of geothermalwater in Henjing, South Jiangxi province, *Hydrogeology and Engineering Geology,* 2001, no. 4, pp. 45–48.

Publisher's Note. Pleiades Publishing remains neutral with regard to jurisdictional claims in published maps and institutional affiliations.
AI tools may have been used in the translation or editing of this article.